

Probing Minimalist Phase Structure in LLMs: What Universal Dependencies Cannot Represent

Yuanhao Chen

Dartmouth College
yc.th@dartmouth.edu

Peter Chin

Dartmouth College
pc@dartmouth.edu

Abstract

Structural probes train on Universal Dependencies (UD), which does not encode formal-syntactic abstractions such as phase boundaries or phase-internal cohesion. Whether large language models (LLMs) encode these remains an open question that UD-based probing cannot answer by construction. We evaluate structural probes on wh-movement stimuli where UD distances are invariant across conditions by design — any non-zero effect therefore reflects structure beyond UD. The three conditions — bare small clause, infinitival, and finite — are ordered by the number of Minimalist Program (MP) phase boundaries the wh-element crosses.

Across 13 LLMs from four families, we find a phase-count gradient on a cross-clause pair (12/13 models) and a 13/13 sign asymmetry on a within-clause pair whose UD distance is identical across conditions — the latter specifically predicted by phase-internal cohesion, an MP abstraction invisible to UD by construction. Activation patching confirms the representations are causally active in 12/13 models. These findings suggest that distributional pre-training can induce representations aligned with formal-syntactic abstractions beyond the reach of annotation-based probing; UD-grounded probes provide a lower bound on syntactic encoding, not an upper bound.

1 Introduction

Structural probing has established that large language models (LLMs) encode syntactic structure in their hidden representations (Hewitt and Manning, 2019; Manning et al., 2020). These probes train on Universal Dependencies (UD) tree distances as the gold target — a consistent, broadly applicable annotation, but not a generative grammar. Whether LLMs encode such formal-syntactic abstractions — phase boundaries, phase-internal cohesion — remains an open question that UD-based probing cannot answer by construction.

This paper evaluates structural probes on wh-movement stimuli constructed so that UD distances are invariant across conditions by design (section 3.1). The three conditions — bare small clause, infinitival, and finite — are ordered by the number of phase boundaries the wh-element crosses, providing a graded test of phase structure in LLM representations.

Across all 13 LLMs from four families, we find that the structural probe distance between an embedded subject and the embedded verb flips sign across conditions: smaller than baseline in the finite condition, larger in the infinitival condition. No surface property predicts this: UD distance between the two words is exactly one edge in every condition, linear word distance predicts no difference for finite (both tokens are adjacent in bare and finite), and a monotone structural-complexity account predicts larger distances in both non-baseline conditions. The pattern is instead predicted by phase-internal cohesion — a Minimalist Program (MP) abstraction invisible to UD by construction (section 4.2) — providing evidence for formal-syntactic representations in LLMs beyond the reach of annotation-based probing.

We make three contributions.

- Phase-structure probing with invariant UD distance.** We design wh-movement stimuli where UD distances are held constant across conditions, ensuring that probe effects reflect structure beyond UD. Across 13 LLMs from four families, we find a phase-count gradient ($\beta_{\text{fin}} > \beta_{\text{inf}} > 0$ in 12/13 models under canonical-layer reporting; sections 3.3 and 4.1) and a 13/13 `ESUBJ-EVB` sign asymmetry — specifically predicted by MP phase structure and inaccessible to any UD-based probe by construction (section 4.2).
- Canonical-layer reporting.** We introduce canonical-layer reporting: anchoring all con-

trasts to the layer that maximises the most reliable contrast, removing a per-contrast degree of freedom that prior structural-probing work has not controlled for. Under this stricter criterion the phase-count gradient holds in 12/13 models; the single failure mode is concealed by per-contrast peak reporting.

- Causal corroboration.** We show that the representations identified by the probe are computationally active: Activation patching at the embedded-subject position shifts probe distances in the predicted direction in 12/13 models, directly addressing the probing-scepticism concern of Agarwal et al. (2025).

2 Background

Phase theory. We treat clause structure in the framework of phase theory (Chomsky, 2000, 2001). A *phase* is a syntactic domain whose complement domain becomes inaccessible to higher derivational operations once the phase is complete. The two phase heads in English are v^0 , the light-verb head projecting a vP, and C, the head of CP. A finite embedded clause therefore introduces two phases (vP and CP) above its embedded verb; an infinitival TP introduces one (vP); a bare small-clause complement introduces no additional phases. The Phase Impenetrability Condition (PIC) restricts cross-phase operations to material at the phase edge (Chomsky, 2001), forcing successive-cyclic wh-movement to transit each phase edge (Urk, 2020). Two predictions from this framework motivate our experimental design. The number of phase boundaries between the wh-position (matrix Spec,CP, after movement) and the base-position wh-copy at the embedded verb’s complement tracks the complement type: bare < infinitival < finite (section 3.1). Arguments inside the same phase are structurally more cohesive than arguments separated by a phase boundary, even when their dependency-tree distance is identical (section 4.2). The first motivates the cross-clause WH-ESUBJ probe pair; the second motivates the within-clause ESUBJ-EVB pair (section 3.1). Table 3 glosses syntactic terms used throughout.

Structural probes. A structural probe is a linear map from a model’s contextualised hidden states to a Euclidean space, trained so that pairwise distances under the probe approximate gold tree distances between words (Hewitt and Manning, 2019; Manning et al., 2020). Our probes are trained on the Universal

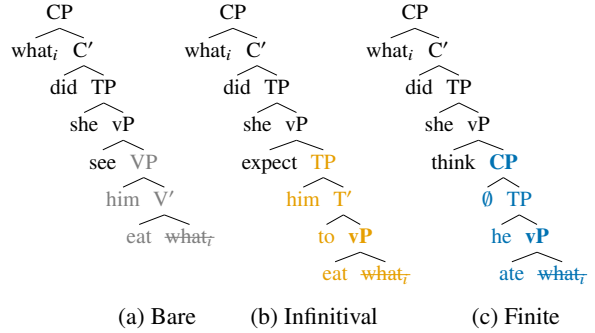


Figure 1: Schematic phrase structures of the three conditions. The embedded clause is colour-coded; phases it introduces are in **bold**, indicating the added phase boundaries: zero for bare (a), one for infinitival (b), two for finite (c). The lower wh-copy is shown struck through at its base position. Intermediate bar levels and matrix projections shared across conditions are omitted; the matrix vP (a phase, but shared) is unbolded. Phrase structures with intermediate projections are in fig. 8.

Dependencies English Web Treebank (UD-EWT) (Silveira et al., 2014) with undirected dependency-tree distance as the gold target. We then evaluate each trained probe on our wh-movement stimuli without further fitting, and report an effect size β : the estimated condition-vs.-bare difference in probe distance for a designated word pair (section 3.2). Because our stimuli are constructed so that UD-tree distance between probed word pairs is invariant across conditions (section 3.1), a non-zero β cannot be a re-encoding of the probe’s training target; it must reflect structural information that UD does not encode. The probing literature has questioned whether what a probe recovers corresponds to what a model computationally uses (Agarwal et al., 2025); we address this directly with the causal-intervention experiment of section 4.3.

3 Stimuli and Methods¹

3.1 Stimuli

Each item is a triple of wh-questions sharing the wh-phrase (*what*), the embedded-subject lemma, and the embedded-verb lemma, with the matrix verb and complement type varying by condition:

- Bare:** What did she see him eat?
Infinitival: What did she expect him to eat?
Finite: What did she think he ate?

The matrix verb is drawn from a condition-

¹Code and stimuli: <https://anonymous.4open.science/r/syntax-probe-147D>.

specific class. The *bare* matrix verb is a perception or causative verb (*see, watch, make, let*) selecting a bare small-clause complement (Stowell, 1981). The *infinitival* matrix is an exceptional case-marking (ECM) or object-control verb (*expect, want, allow, need*) selecting an infinitival TP complement (Chomsky, 1986). The *finite* matrix is a bridge verb (*think, believe, claim, say, know, suppose, report*) selecting a finite CP complement with a null complementizer (Erteschik-Shir, 1973). In the bare and infinitival conditions the embedded subject bears accusative case and the embedded verb appears in its base form; in the finite condition the embedded subject bears nominative case and the embedded verb appears in the simple past.

The three conditions are ordered by complement size (fig. 1): bare small clause < infinitival TP < finite CP, equivalently an ordering by number of phase boundaries crossed along the wh-movement path (Chomsky, 2000, 2001). We treat bare as the structural baseline: A contrast against bare measures the representational consequences of the additional clause structure.

We tag three positions per stimulus — wh, embedded_subject, embedded_verb — and measure two probe distances: WH-ESUBJ (wh-element to embedded subject), capturing cross-clause structural depth as a function of complement type; and ESUBJ-EVB (embedded subject to embedded verb), capturing within-clause cohesion.

UD-distance invariance. For probe-distance differences to be interpretable, the UD-tree distance between each probe pair must be constant across conditions within each item; otherwise differences in β would be confounded with UD-level differences. We parse every stimulus with spaCy’s en_core_web_trf model (RoBERTa-based, self-reported LAS ≈ 94 on its OntoNotes-derived eval, with UD-converted output schema; Honnibal et al., 2020) and verify within-item invariance. By design, ESUBJ-EVB is exactly 1 edge (nsubj) in every condition. WH-ESUBJ varies by at most 1 edge in a minority of items, where the parser assigns a *shorter* UD path in the infinitival than in bare. Since our prediction is that probe distance *increases* with structural depth, this directional mismatch cannot manufacture the predicted effect.

Lexicon and item generation. The combinatorial lexicon comprises 7 matrix subjects, 7 embedded subjects (in matched accusative/nominative pairs), 4 bare-class matrix verbs, 4 infinitival-class

verbs, 7 bridge verbs, and 20 embedded transitive verbs with inanimate-compatible objects. Items are constrained so that the matrix and embedded subjects differ and so that the three matrix verbs are mutually distinct within an item. The Cartesian product yields on the order of 10^5 candidate items; we use a fixed seed-controlled sample of 1,000 items, yielding 3,000 stimuli (one per condition per item).

3.2 Probing Setup

Probe training. We follow the structural-probe protocol of Hewitt and Manning (2019). For each transformer layer ℓ , we obtain a per-word representation $h_w^{(\ell)} \in \mathbb{R}^d$ by mean-pooling the subword-token hidden states at layer ℓ for each word w (d is the model’s hidden size). We then train a linear projection $B^{(\ell)} \in \mathbb{R}^{r \times d}$ with $r = 64$, defining the probe distance between any two words u, v at layer ℓ as

$$d_B^{(\ell)}(u, v) := \|B^{(\ell)}(h_u^{(\ell)} - h_v^{(\ell)})\|_2^2,$$

the squared L2 norm of the projected difference (Hewitt and Manning, 2019, eq. 1). $B^{(\ell)}$ is fit by minimising L1 loss between $d_B^{(\ell)}(u, v)$ and the gold undirected dependency-tree distance between u, v on the UD-EWT training corpus (Silveira et al., 2014), using Adam (learning rate 10^{-3} , batch size 256) for up to 100 epochs with learning-rate decay on plateau (factor 0.1, patience 1, up to 4 resets). Input activations are standardised per training corpus before projection. The resulting per-layer probes are then evaluated on our wh-movement stimuli without further fitting.

Effect-size estimation. For each (model, layer ℓ , pair) we fit one treatment-coded ordinary least squares (OLS) regression

$$d_{i,k}^{(\ell)} = \beta_0^{(\ell)} + \beta_{\text{fin}}^{(\ell)} \cdot \mathbb{1}[c_{i,k} = \text{fin}] + \beta_{\text{inf}}^{(\ell)} \cdot \mathbb{1}[c_{i,k} = \text{inf}] + \varepsilon_{i,k}^{(\ell)},$$

where $d_{i,k}^{(\ell)}$ is the probe distance $d_B^{(\ell)}$ for the relevant word pair in stimulus k of item i , $c_{i,k}$ is the condition, $\mathbb{1}[\cdot]$ is the indicator function, $\varepsilon_{i,k}^{(\ell)}$ is the error term, and bare is the reference category (so $\beta_0^{(\ell)}$ is the bare-condition mean probe distance). Standard errors are cluster-robust at the item level, accounting for the within-item correlation produced by three stimuli per item. The headline coefficients are the contrast slopes $\beta_{\text{fin}}^{(\ell)}$ (finite – bare) and $\beta_{\text{inf}}^{(\ell)}$ (infinitival – bare). We

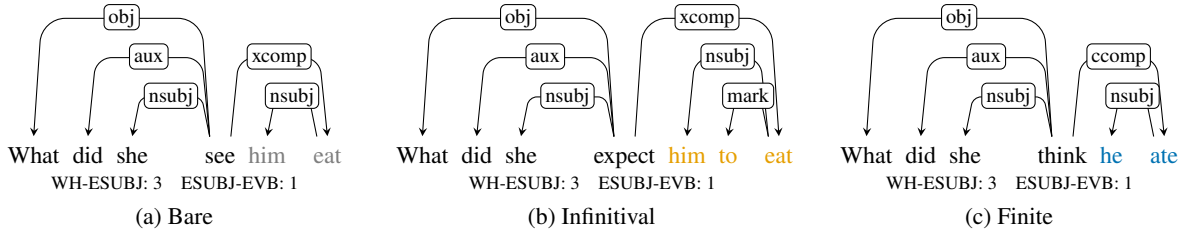


Figure 2: UD parses of the three conditions, with embedded-clause words colour-coded by condition (matching fig. 1). Within-item UD-tree distances for the two probe pairs are invariant across conditions: 3 edges for WH-ESUBJ (*what* \leftrightarrow *him/he*) and 1 edge for ESUBJ-EVB (*him/he* \leftrightarrow *eat/ate*). Any non-zero β on either pair therefore reflects structural information beyond UD.

apply Benjamini–Hochberg false discovery rate (FDR) correction (Benjamini and Hochberg, 1995) across all (layer \times pair \times contrast) tests within each model. For point-magnitude reporting in figures we additionally compute non-parametric 95% confidence intervals (CIs) by cluster bootstrap on item id ($n = 1000$ resamples, percentile method); the bootstrap operates on the raw contrast mean-difference $\bar{d}_{\text{target}} - \bar{d}_{\text{bare}}$ and is independent of the OLS fit.

Stimulus-verification filter. Items failing the UD-distance invariance check (section 3.1) for a given probe pair are excluded from both the regression and the bootstrap for that pair, preventing residual UD-level variance from contributing to β .

3.3 Canonical-Layer Reporting

A common shortcut in the structural-probing literature is to report the per-model layer maximum $\beta^{\text{peak}} = \max_{\ell} \beta^{(\ell)}$ (Hewitt and Manning, 2019; Manning et al., 2020); when multiple contrasts are involved, this extends to selecting the peak layer independently for each. This summary is opportunistic when the per-contrast maxima land at different layers — in our panel, 0 of 13 models share the same peak layer for β_{fin} and β_{inf} on the WH-ESUBJ pair, so per-contrast peak reporting always selects a different layer for the two contrasts.

We therefore define a single *canonical layer* per model, anchored to the more robust contrast:

$$L^* := \arg \max_{\ell} \beta_{\text{fin}}^{(\ell)},$$

and report the canonical-layer estimate $\beta^{\text{canon}} := \beta^{(L^*)}$ for both contrasts at L^* . Anchoring on finite reflects empirical reliability: β_{fin} is reliably positive across the panel (section 4.1), whereas β_{inf} is sparser and noisier and is precisely the contrast for which we wish to remove a degree of freedom.

By construction $\beta_{\text{fin}}^{\text{canon}} = \beta_{\text{fin}}^{\text{peak}}$; $\beta_{\text{inf}}^{\text{canon}}$ may be substantially smaller than $\beta_{\text{inf}}^{\text{peak}}$. Canonical-layer

reporting is a strict refinement of peak reporting: Any claim it makes about β_{inf} also holds for $\beta_{\text{inf}}^{\text{peak}}$, but the converse fails. Where the converse fails (e.g. Qwen-3-4B; section 4.1), peak reporting conceals heterogeneity that canonical-layer reporting surfaces.

3.4 Models

We evaluate on 13 decoder-only language models from four families: Gemma-3 (Team et al., 2025), Llama-3 (Grattafiori et al., 2024), Mistral (Jiang et al., 2023), and Qwen (Qwen et al., 2025; Yang et al., 2025). All models are base (non-instruction-tuned) pretrained checkpoints, accessed via the HuggingFace Transformers library; the full panel is in table 2. Probe training and evaluation were run on a single NVIDIA RTX PRO 6000 Blackwell GPU; total wall-clock time was under two hours.

4 Experiments

4.1 Cross-Clause Depth: The Phase-Count Gradient

We probe each of 13 LLMs on the wh-movement stimuli (section 3.1) and estimate $\beta_{\text{fin}}^{(\ell)}$ and $\beta_{\text{inf}}^{(\ell)}$ on the WH-ESUBJ pair across all transformer layers. Figure 3 gives per-model layer profiles, fig. 4 compares per-contrast peak vs. canonical-layer reporting, and table 1 reports per-model headline numbers. The within-clause ESUBJ-EVB pair is treated separately in section 4.2.

The phase-count gradient under peak vs. canonical reporting. At the per-contrast peak layer, all 13 models show the predicted gradient $\beta_{\text{fin}} > \beta_{\text{inf}} > 0$ on the WH-ESUBJ pair,² with median panel ratio

²The basis for $\beta_{\text{inf}} > 0$ is indirect: Phrase-structure distance from wh to the embedded subject is equal in bare and infinitival. The distinction is derivational — the infinitival subject is base-merged at Spec,v*P (phase edge; fig. 8; Chomsky 2001) while the bare subject is at Spec,VP (non-phase).

$\beta_{\text{fin}}^{\text{peak}}/\beta_{\text{inf}}^{\text{peak}} \approx 2.18$. This summary is, however, sensitive to layer choice: None of the 13 models share the same peak layer for β_{fin} and β_{inf} . Under canonical-layer reporting (section 3.3), the gradient prediction holds in 12 of 13 models: $\beta_{\text{inf}}^{\text{canon}} > 0$ in the predicted direction, and 9 of 13 satisfy $\beta_{\text{inf}}^{\text{canon}} > +0.1$ (table 1). The median panel β_{inf} drops from +0.37 at per-contrast peak to +0.17 at canonical layer, while the median β_{fin} is unchanged by construction; the median $\beta_{\text{fin}}/\beta_{\text{inf}}$ ratio rises from ≈ 2.2 to ≈ 5.1 . The infinitival signal is therefore more layer-localised than the finite signal: It attenuates substantially at L^* relative to its own peak (fig. 4). Section E confirms the gradient direction holds under two additional metrics: the layer median and the fraction of FDR-significant positive layers.

The one canonical-layer failure. Qwen-3-4B is the sole canonical-layer failure on WH-ESUBJ: Its β_{fin} peaks at layer 10, where $\beta_{\text{inf}}^{\text{canon}} = -0.045$ (a sign reversal at L^*), while β_{inf} has its own peak at layer 4 (+0.34). The methodology thus surfaces a discrepancy that per-contrast peak reporting would have hidden.

Per-layer reliability of the finite signal. On WH-ESUBJ, $\beta_{\text{fin}}^{\text{canon}}$ ranges from +0.55 (Gemma-3-1B) to +0.99 (Gemma-3-27B); the panel median of FDR-significant positive layers for β_{fin} is 94%, five of 13 models reach $\geq 97\%$, and the lowest is Gemma-3-1B at 63%. The finite-bare contrast is therefore a broad layer-wise signal rather than a single-layer peak. Within-family scaling is heterogeneous: The Gemma family scales monotonically with size (+0.55, +0.91, +0.96, +0.99 at 1B, 4B, 12B, 27B) but the Llama family does not (Llama-3.2-1B at +0.77 exceeds Llama-3.1-8B at +0.72).

4.2 Within-Clause Cohesion: The Sign Asymmetry

We turn from the cross-clause pair to the within-clause pair: the embedded subject and the embedded verb (ESUBJ-EVB), whose UD-tree distance is exactly 1 edge (nsubj) in every condition by design (fig. 2). The empirical finding is a robust sign asymmetry: In every one of the 13 models, across all four architecture families, $\beta_{\text{fin}}^{\text{peak}} < 0$ and $\beta_{\text{inf}}^{\text{peak}} > 0$ on ESUBJ-EVB, with peak magnitudes typically in the 0.3–0.6 range (fig. 5, with per-model layer profiles in fig. 6). Since the two contrasts have opposite predicted signs, canonical-layer reporting (section 3.3) does not apply here.

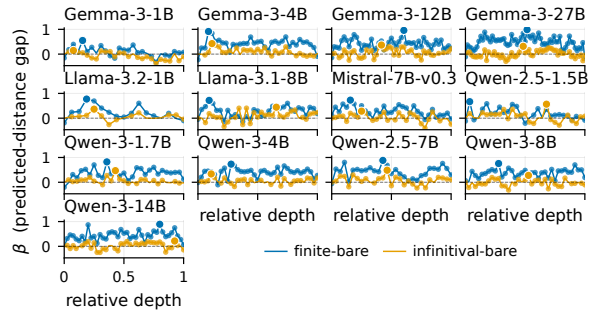


Figure 3: Per-model layer profiles of $\beta_{\text{fin}}^{(\ell)}$ (finite – bare) and $\beta_{\text{inf}}^{(\ell)}$ (infinitival – bare) on the WH-ESUBJ pair. Small filled markers indicate layers FDR-significant at $\alpha = 0.05$; the larger white-edged marker is the per-contrast peak in the predicted direction.

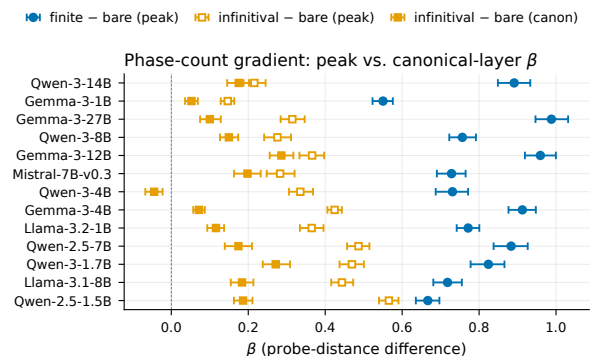


Figure 4: Per-model peak vs. canonical-layer β on the WH-ESUBJ pair, with 95% cluster-bootstrap CIs. β_{fin} is shown at its peak layer (= canonical by construction). β_{inf} is shown both at its own peak (open markers) and at L^* (filled markers).

Three observations rule out simpler accounts.

First, UD distance between the two words is 1 edge in every condition (fig. 2), so a pure UD-decoding probe would yield $\beta \approx 0$. Second, the linear distance between the two words is 1 word in bare and finite but 2 words in infinitival (the *to* marker intervenes). A surface-linear-distance heuristic predicts $\beta_{\text{inf}} > 0$ and $\beta_{\text{fin}} \approx 0$; the observed *negative* β_{fin} cannot come from linear distance. Third, a monotone structural-complexity heuristic — “more structure between the two words means larger probe distance” — predicts $\beta_{\text{fin}} > \beta_{\text{inf}} > 0$, since finite adds the most structure and bare the least. The observed *negative* β_{fin} directly contradicts this prediction.

Per-layer pattern. The sign asymmetry is not a single-layer peak. Layer profiles (fig. 6) show $\beta_{\text{fin}} < 0$ and $\beta_{\text{inf}} > 0$ at FDR-significant layers throughout most of the network in most models. As with the cross-clause finding, the pattern holds across all four architecture families.

Table 1: Phase-count-gradient summary at canonical-layer reporting, on the WH-ESUBJ pair. L^* is the canonical layer (the layer maximising β_{fin}). The two β columns give the bootstrap-mean effect at L^* with 95% cluster-bootstrap CIs. “FDR+ layers” counts the layers at which the OLS estimate of β_{fin} on WH-ESUBJ is positive and significant under Benjamini–Hochberg correction at $\alpha = 0.05$.

Model	L^*	$\beta_{\text{fin}}^{\text{canon}}$ (95% CI)	$\beta_{\text{inf}}^{\text{canon}}$ (95% CI)	FDR+ layers
Gemma-3-1B	4	+0.550 (+0.52, +0.58)	+0.052 (+0.04, +0.07)	17/27 (63%)
Gemma-3-4B	3	+0.912 (+0.88, +0.95)	+0.072 (+0.06, +0.09)	33/35 (94%)
Gemma-3-12B	29	+0.959 (+0.92, +1.00)	+0.286 (+0.26, +0.32)	48/49 (98%)
Gemma-3-27B	32	+0.988 (+0.95, +1.03)	+0.100 (+0.07, +0.13)	61/63 (97%)
Llama-3.2-1B	3	+0.772 (+0.74, +0.80)	+0.116 (+0.09, +0.14)	13/17 (76%)
Llama-3.1-8B	3	+0.718 (+0.68, +0.76)	+0.184 (+0.15, +0.21)	28/33 (85%)
Mistral-7B-v0.3	5	+0.728 (+0.69, +0.76)	+0.198 (+0.16, +0.23)	30/33 (91%)
Qwen-2.5-1.5B	1	+0.667 (+0.64, +0.70)	+0.186 (+0.16, +0.21)	20/29 (69%)
Qwen-3-1.7B	10	+0.824 (+0.78, +0.87)	+0.271 (+0.24, +0.31)	27/29 (93%)
Qwen-3-4B	10	+0.731 (+0.69, +0.77)	-0.045 (-0.07, -0.02)	35/37 (95%)
Qwen-2.5-7B	12	+0.883 (+0.84, +0.93)	+0.174 (+0.14, +0.21)	28/29 (97%)
Qwen-3-8B	10	+0.756 (+0.72, +0.79)	+0.150 (+0.13, +0.17)	36/37 (97%)
Qwen-3-14B	32	+0.891 (+0.85, +0.93)	+0.175 (+0.15, +0.20)	40/41 (98%)

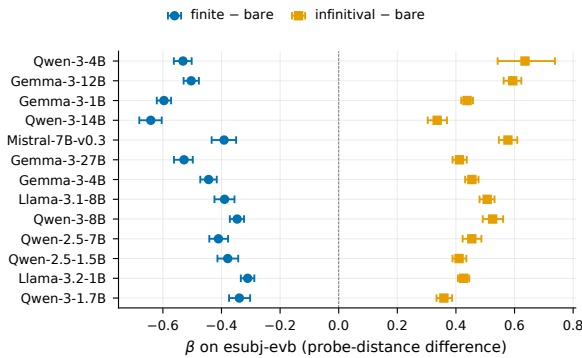


Figure 5: Per-model peak β on the ESUBJ-EVB pair with 95% cluster-bootstrap CIs. All 13 models show $\beta_{\text{fin}}^{\text{peak}} < 0$ and $\beta_{\text{inf}}^{\text{peak}} > 0$ — a 13/13 sign asymmetry. β_{fin} is shown at its predicted-direction peak ($\arg \min_{\ell} \beta_{\text{fin}}^{(\ell)}$); β_{inf} at its peak ($\arg \max_{\ell} \beta_{\text{inf}}^{(\ell)}$). Models are ordered by the magnitude of the asymmetry ($\beta_{\text{inf}}^{\text{peak}} - \beta_{\text{fin}}^{\text{peak}}$), descending.

From the PIC to representations. The PIC (Chomsky, 2000, 2001) is a constraint on syntactic derivation — it determines which operations the grammar can perform across phase boundaries — and is not, in itself, a claim about representational geometry. To connect phase theory to the observed sign asymmetry we therefore need an additional assumption. The candidate is phase-internal cohesion: Items inside the same completed phase are spelled out as a unit and share locality-domain status, leading to more shared computation than structural depth alone predicts and making them

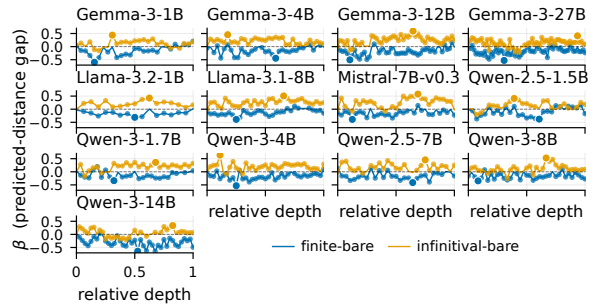


Figure 6: Per-model layer profiles of $\beta_{\text{fin}}^{(\ell)}$ (finite – bare) and $\beta_{\text{inf}}^{(\ell)}$ (infinitival – bare) on the ESUBJ-EVB pair. The sign asymmetry — $\beta_{\text{fin}} < 0$ and $\beta_{\text{inf}} > 0$ — holds at FDR-significant layers throughout most of the network in most models. Marker conventions follow fig. 3.

representationally closer in the model’s hidden states.

Three converging lines of work. The cohesion hypothesis is supported by independent strands of evidence. Multiple-Spell-Out models (Uriagereka, 1999, 2012; Fox and Pesetsky, 2005) treat derivation as cyclic spell-out domains dispatched to the interfaces as units. The locality-domain literature (Müller, 2011; Bošković, 2007; Lee-Schoenfeld, 2008; Canac Marquis, 2005) treats phases as the domains for agreement, case, and binding, within which items remain mutually accessible. And sentence-processing work has found that comprehenders perform additional integrative computation at clause boundaries (Just and Carpenter, 1980;

Rayner et al., 2000), consolidating within-clause material into a unitary representation — a clause-wrap-up effect that is not directly about phases but aligns with the cohesion intuition. None of these directly establishes phase-internal cohesion as an empirical fact about LLMs, but each provides a converging reason to expect within-phase material to be represented as a more cohesive unit than cross-phase material.

Why ESUBJ-EVB specifically. Phase cohesion would in principle apply to any pair of items inside the same phase. Its predictive force is asymmetric across our two probe pairs for a structural reason. For ESUBJ-EVB , both items sit inside the embedded clause: In the finite condition both are inside a complete CP phase, while in the infinitival and bare conditions the embedded clause is not itself a phase. Phase cohesion therefore applies only in the finite condition, predicting that finite tightens the pair representationally relative to bare — exactly the observed $\beta_{\text{fin}} < 0$. For WH-ESUBJ , the items span clause boundaries and are never co-internal to any embedded phase; phase cohesion does not apply.

The phase-cohesion reading predicts the observed direction: Finite couples the embedded subject and verb most tightly (both inside one phase; $\beta_{\text{fin}} < 0$ against the no-phase baseline); infinitival splits them across a phase boundary (separately spelled out; $\beta_{\text{inf}} > 0$). We treat phase cohesion as one possible account among others. The strong empirical claim is the 13/13 sign asymmetry itself, which no UD-, linear-, or monotone-complexity-based account predicts.

4.3 Causal Experiment: Embedded-Subject Patching

The cross-clause and within-clause results (sections 4.1 and 4.2) establish that LLM representations exhibit correlates of phase structure. This is observational evidence: It does not establish that those representations are causally used in the model’s computation. The probing literature has raised this concern in general terms (Agarwal et al., 2025); we address it directly with an activation-patching experiment.

Design. For each item, we pair a source condition (infinitival) and a target condition (bare). The source and target share lexical content but differ in the embedded clause — *She expected him to leave* versus *She saw him leave*. At each model’s

canonical layer L^* (table 1), we replace the residual-stream representation at the embedded subject’s first subword token with the source representation; the probe re-pools across all subwords (section 3.2), so the patch contributes proportionally to the word’s pooled representation. We measure the resulting change $\Delta\beta = \beta_{\text{patched}} - \beta_{\text{target}}$ on the WH-ESUBJ pair. We use (infinitival, bare) rather than (finite, bare): The infinitival adds only T and a vP shell above the bare baseline, isolating the structural-depth manipulation, whereas (finite, bare) additionally conflates morphological finiteness, the complementizer, and agreement. As a negative control, we additionally patch at the wh-position (matrix Spec,CP) and measure $\Delta\beta$ on WH-ESUBJ . The wh-element’s local representation should not directly encode embedded-clause structure, so this should yield $|\Delta\beta| \approx 0$ — a test against generic artefacts of the patching procedure.

Predictions. If the embedded subject’s representation causally encodes the clause-type information picked up by the probe, patching the infinitival’s representation into the bare target should yield $\Delta\beta > 0$ on WH-ESUBJ with bootstrap 95% CI excluding zero. The wh-position control should yield $|\Delta\beta| \leq 0.05$.

Results. Twelve of 13 models show positive $\Delta\beta$ on WH-ESUBJ with bootstrap 95% CI excluding zero (point estimates +0.08–+0.40); the exception is Qwen-3-4B (point estimate –0.06; CI includes zero), the same model that fails canonical-layer reporting in section 4.1. The wh-position control yields $|\Delta\beta| \leq 0.05$ in 12 of 13 models; the exception is Qwen-2.5-7B at $|\Delta\beta| = 0.060$, marginally above the threshold. These near-null control results support the interpretation that the headline effect is not a generic patching artefact (fig. 7).

Scope of the causal claim. The intervention sits on the embedded subject’s residual stream, and probe distances for the within-clause ESUBJ-EVB pair are consequently affected too (fig. 7, right panel). We therefore read the result conservatively: The embedded subject’s representation causally encodes clause-type information in a way that affects every probe pair containing that word, rather than being specific to the cross-clause structural depth. The experiment does not directly test the ESUBJ-EVB sign asymmetry, which spans all three conditions and is not reducible to single-word encoding.

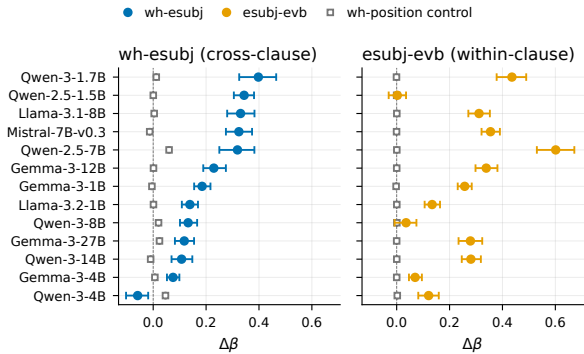


Figure 7: Per-model $\Delta\beta$ for the embedded-subject patch (filled circles) and the wh-position negative control (open grey squares), measured on WH-ESUBJ (left panel, blue) and ESUBJ-EVB (right panel, orange). Source condition is infinitival; target is bare; intervention layer is each model’s canonical layer L^* . Bootstrap 95% CIs shown.

5 Related Work

The structural probe (Hewitt and Manning, 2019; Manning et al., 2020) casts syntactic encoding as a linear transformation of contextualised word representations trained to recover UD dependency-tree distances. Because probe training and evaluation both operate within the UD framework, structural probing is by construction sensitive only to UD-grounded distinctions. Kennedy (2025) extend the structural probe to generative-syntax stimuli contrasting subject-raising and subject-control structures, providing the closest precedent for evaluating structural probes against distinctions that UD does not directly encode. The present work strengthens this test: UD-tree distances between probed pairs are invariant across conditions by construction, verified per item, so no residual UD difference can account for observed effects.

A parallel tradition uses behavioural evaluations — minimal-pair acceptability contrasts — to assess syntactic knowledge in language models. Marvin and Linzen (2018) established a broad-coverage evaluation spanning agreement, reflexive anaphora, and negative-polarity phenomena. For wh-movement specifically, Wilcox et al. (2018) showed that RNN models track gap sites but fail on island constraints; Koo and Kim (2026) extended this to GPT-style Transformer models, finding failure to replicate human sensitivity to successive-cyclic movement. Behavioural and representational methods are not interchangeable: Agarwal et al. (2025) demonstrate across 32 models that structural probe accuracy does not predict minimal-pair performance, indicating that the two approaches

recover different aspects of syntactic knowledge.

Whether probed representations play a causal role in model computation — rather than merely correlating with behaviour — is a central methodological concern (Agarwal et al., 2025), formalised in the causal-abstraction framework of Geiger et al. (2023). Activation patching tests this directly: An internal representation is replaced with one from a counterfactual input, and the downstream change in the probed quantity measures causal relevance.

6 Discussion

Structural encoding below the UD surface. The ESUBJ-EVB sign asymmetry — $\beta_{\text{fin}}^{\text{peak}} < 0$ and $\beta_{\text{inf}}^{\text{peak}} > 0$ across all 13 models — is the central existence proof that LLM representations encode structural information inaccessible to UD-grounded probing. Three alternative accounts — UD-distance-based, surface-linear, and monotone-complexity-based — all fail to account for the sign asymmetry (section 4.2). The pattern is specifically predicted by phase-internal cohesion — a formal-syntactic abstraction from the MP’s treatment of cyclic spell-out, invisible to UD by construction. Its 13/13 replication across four architectures suggests that distributional pretraining can induce representations aligned with formal-syntactic abstractions beyond the reach of annotation-based probing. The implication is as methodological as it is empirical: UD-grounded probes provide a lower bound on syntactic encoding, not an upper bound.

Canonical-layer reporting. Anchoring all contrasts to L^* (the layer maximising the most reliable contrast) removes one cross-contrast degree of freedom and makes canonical-layer claims strictly stronger than per-contrast peak claims. We recommend canonical-layer reporting as a default for structural-probing work that compares multiple contrasts in the same predicted direction over a shared model panel.

Causal corroboration and its scope. The activation-patching result (section 4.3) places the phase-count gradient on causal footing: The embedded subject’s representation is not merely correlated with clause-type information but encodes it in a way that shapes the model’s internal distances. The scope is conservative — the intervention sits on a single word’s residual stream — but the result directly addresses the probing-scepticism concern of Agarwal et al. (2025).

Limitations

All stimuli and probes are in English. The theoretical predictions follow from phase structure, which generalises cross-linguistically, but the specific three-way complement-size contrast exploits English-specific verb-class properties and case morphology. Extension to languages with overt morphological or word-order diagnostics for phase structure — such as V2 languages, where finite verbs obligatorily move to C in main clauses, or ergative languages with distinct case-phase interactions — would provide a more stringent cross-linguistic test.

The phase-count gradient prediction is directional: We predict $\beta_{\text{fin}}^{\text{canon}} > \beta_{\text{inf}}^{\text{canon}} > 0$ but make no prediction about the ratio’s magnitude; the prediction holds for any $\beta_{\text{fin}}^{\text{canon}}/\beta_{\text{inf}}^{\text{canon}} > 1$. Qwen-3-4B is the sole canonical-layer failure; we have no principled account of why this model differs from the other twelve. Within-family scaling on β_{fin} is heterogeneous across the panel (section 4.1), and what determines the $\beta_{\text{fin}}/\beta_{\text{inf}}$ ratio magnitude remains an open question.

The panel covers 13 publicly available base models from four architecture families, with parameter counts between 1B and 27B. It excludes instruction-tuned variants, mixture-of-experts models, and models above 27B; whether the phase-count gradient and the ESUBJ-EVB sign asymmetry extend to these settings is unknown.

Acknowledgments

This research was funded by the Defense Advanced Research Projects Agency (DARPA), under contract W912CG23C0031.

References

- Ananth Agarwal, Jasper Jian, Christopher D Manning, and Shikhar Murty. 2025. [Mechanisms vs. Outcomes: Probing for Syntax Fails to Explain Performance on Targeted Syntactic Evaluations](#). In *Proceedings of the 2025 Conference on Empirical Methods in Natural Language Processing*, pages 33737–33757, Suzhou, China. Association for Computational Linguistics.
- Yoav Benjamini and Yosef Hochberg. 1995. [Controlling the False Discovery Rate: A Practical and Powerful Approach to Multiple Testing](#). *Journal of the Royal Statistical Society: Series B (Methodological)*, 57(1):289–300.
- Željko Bošković. 2007. [On the Locality and Motivation of Move and Agree: An Even More Minimal Theory](#). *Linguistic Inquiry*, 38(4):589–644.
- Rejean Canac Marquis. 2005. [Phases and Binding of Reflexives and Pronouns in English](#). *Proceedings of the International Conference on Head-Driven Phrase Structure Grammar*.
- Noam Chomsky. 1986. *Barriers*. Linguistic Inquiry Monographs. MIT Press, Cambridge, MA, USA.
- Noam Chomsky. 2000. Minimalist Inquiries: The Framework. In *Step by Step: Essays on Minimalist Syntax in Honor of Howard Lasnik*, pages 89–155. MIT Press, Cambridge.
- Noam Chomsky. 2001. [Derivation by Phase](#). In Michael Kenstowicz, editor, *Ken Hale*, pages 1–52. The MIT Press.
- Nomi Erteschik-Shir. 1973. [On the nature of island constraints](#). Ph.D. thesis, Massachusetts Institute of Technology.
- Danny Fox and David Pesetsky. 2005. [Cyclic Linearization of Syntactic Structure](#). *Theoretical Linguistics*, 31(1-2):1–45.
- Atticus Geiger, Duligur Ibeling, Amir Zur, Maheep Chaudhary, Sonakshi Chauhan, Jing Huang, Aryaman Arora, Zhengxuan Wu, Noah Goodman, Christopher Potts, and Thomas Icard. 2023. [Causal Abstraction: A Theoretical Foundation for Mechanistic Interpretability](#).
- Aaron Grattafiori, Abhimanyu Dubey, Abhinav Jauhri, Abhinav Pandey, Abhishek Kadian, Ahmad Al-Dahle, Aiesha Letman, Akhil Mathur, Alan Schelten, Alex Vaughan, Amy Yang, Angela Fan, Anirudh Goyal, Anthony Hartshorn, Aobo Yang, Archi Mitra, Archie Sravankumar, Artem Korenev, Arthur Hinsvark, and 542 others. 2024. [The Llama 3 Herd of Models](#). *arXiv preprint*. ArXiv:2407.21783 [cs.AI].
- John Hewitt and Christopher D. Manning. 2019. [A Structural Probe for Finding Syntax in Word Representations](#). In *Proceedings of the 2019 Conference of the North American Chapter of the Association for Computational Linguistics: Human Language Technologies, Volume 1 (Long and Short Papers)*, pages 4129–4138, Minneapolis, Minnesota. Association for Computational Linguistics.
- Matthew Honnibal, Ines Montani, Sofie Van Landeghem, and Adriane Boyd. 2020. [spaCy: Industrial-strength natural language processing in python](#).
- Albert Q. Jiang, Alexandre Sablayrolles, Arthur Mensch, Chris Bamford, Devendra Singh Chaplot, Diego de las Casas, Florian Bressand, Gianna Lengyel, Guillaume Lample, Lucile Saulnier, L  lio Renard Lavaud, Marie-Anne Lachaux, Pierre Stock, Teven Le Scao, Thibaut Lavril, Thomas Wang, Timoth  e Lacroix, and William El Sayed. 2023. [Mistral 7B](#). *arXiv preprint*. ArXiv:2310.06825 [cs.CL].
- Marcel A. Just and Patricia A. Carpenter. 1980. [A theory of reading: From eye fixations to comprehension](#). *Psychological Review*, 87(4):329–354.

- Mary Kennedy. 2025. [Evidence of Generative Syntax in LLMs](#). In *Proceedings of the 29th Conference on Computational Natural Language Learning*, pages 377–396, Vienna, Austria. Association for Computational Linguistics.
- Keonwoo Koo and Hyosik Kim. 2026. [Successive-cyclic movement in humans and neural language models: testing wh-filler-gap dependencies](#). *Frontiers in Psychology*, 16.
- Vera Lee-Schoenfeld. 2008. [Binding, Phases, and Locality](#). *Syntax*, 11(3):281–298.
- Christopher D. Manning, Kevin Clark, John Hewitt, Urvashi Khandelwal, and Omer Levy. 2020. [Emergent linguistic structure in artificial neural networks trained by self-supervision](#). *Proceedings of the National Academy of Sciences*, 117(48):30046–30054.
- Rebecca Marvin and Tal Linzen. 2018. [Targeted Syntactic Evaluation of Language Models](#). In *Proceedings of the 2018 Conference on Empirical Methods in Natural Language Processing*, pages 1192–1202, Brussels, Belgium. Association for Computational Linguistics.
- Gereon Müller. 2011. [Constraints on Displacement: A phase-based approach](#), volume 7 of *Language Faculty and Beyond*. John Benjamins Publishing Company, Amsterdam.
- Qwen, An Yang, Baosong Yang, Beichen Zhang, Binyuan Hui, Bo Zheng, Bowen Yu, Chengyuan Li, Dayiheng Liu, Fei Huang, Haoran Wei, Huan Lin, Jian Yang, Jianhong Tu, Jianwei Zhang, Jianxin Yang, Jiayi Yang, Jingren Zhou, Junyang Lin, and 24 others. 2025. [Qwen2.5 Technical Report](#). *arXiv preprint*. ArXiv:2412.15115 [cs.CL].
- Keith Rayner, Gretchen Kambe, and Susan A. Duffy. 2000. [The Effect of Clause Wrap-Up on Eye Movements during Reading](#). *The Quarterly Journal of Experimental Psychology Section A*, 53(4):1061–1080.
- Natalia Silveira, Timothy Dozat, Marie-Catherine de Marneffe, Samuel R. Bowman, Miriam Connor, John Bauer, and Chris Manning. 2014. [A gold standard dependency corpus for English](#). In *Proceedings of the Ninth International Conference on Language Resources and Evaluation (LREC’14)*, pages 2897–2904, Reykjavik, Iceland. European Language Resources Association (ELRA).
- Timothy Angus Stowell. 1981. [Origins of phrase structure](#). Thesis, Massachusetts Institute of Technology. Accepted: 2009-01-23T14:40:10Z.
- Gemma Team, Aishwarya Kamath, Johan Ferret, Shreya Pathak, Nino Vieillard, Ramona Merhej, Sarah Perrin, Tatiana Matejovicova, Alexandre Ramé, Morgane Rivière, Louis Rouillard, Thomas Mesnard, Geoffrey Cideron, Jean-bastien Grill, Sabela Ramos, Edouard Yvinec, Michelle Casbon, Etienne Pot, Ivo Penchev, and 197 others. 2025. [Gemma 3 Technical Report](#). *arXiv preprint*. ArXiv:2503.19786 [cs.CL].
- Juan Uriagereka. 1999. [Multiple Spell-Out](#). In *Working Minimalism*. The MIT Press.
- Juan Uriagereka. 2012. [Spell-out and the minimalist program](#). Oxford linguistics. Oxford university press, Oxford New York.
- Coppe van Urk. 2020. [Successive Cyclicity and the Syntax of Long-Distance Dependencies](#). *Annual Review of Linguistics*, 6(Volume 6, 2020):111–130.
- Ethan Wilcox, Roger Levy, Takashi Morita, and Richard Futrell. 2018. [What do RNN Language Models Learn about Filler–Gap Dependencies?](#) In *Proceedings of the 2018 EMNLP Workshop BlackboxNLP: Analyzing and Interpreting Neural Networks for NLP*, pages 211–221, Brussels, Belgium. Association for Computational Linguistics.
- An Yang, Anfeng Li, Baosong Yang, Beichen Zhang, Binyuan Hui, Bo Zheng, Bowen Yu, Chang Gao, Chengen Huang, Chenxu Lv, Chujie Zheng, Dayiheng Liu, Fan Zhou, Fei Huang, Feng Hu, Hao Ge, Haoran Wei, Huan Lin, Jialong Tang, and 41 others. 2025. [Qwen3 Technical Report](#). *arXiv preprint*. ArXiv:2505.09388 [cs.CL].

A Full Model Panel

Table 2 lists all 13 models with their family, parameter count, and number of transformer blocks. All models are used under licenses permitting academic research use: the Gemma Terms of Use (Gemma-3), the Meta Llama 3 Community License (Llama-3), and Apache 2.0 (Mistral-7B-v0.3, Qwen-2.5, Qwen-3).

Table 2: The 13-model panel, organised by family. “Layers” is the number of transformer blocks, excluding the embedding layer.

Family	Model	Size	Layers
Gemma-3	Gemma-3-1B	1B	26
	Gemma-3-4B	4B	34
	Gemma-3-12B	12B	48
	Gemma-3-27B	27B	62
Llama-3	Llama-3.2-1B	1B	16
	Llama-3.1-8B	8B	32
Mistral	Mistral-7B-v0.3	7B	32
Qwen	Qwen2.5-1.5B	1.5B	28
	Qwen2.5-7B	7B	28
	Qwen3-1.7B	1.7B	28
	Qwen3-4B	4B	36
	Qwen3-8B	8B	36
	Qwen3-14B	14B	40

B Syntactic Terminology

Table 3 defines the syntactic terms used throughout the paper.

Table 3: Syntactic terms used in the paper.

Term	Description
X, X', XP	X-bar notation: X is the head, X' (X-bar) is the intermediate projection combining the head with its complement(s), and XP is the maximal phrase (e.g. CP, TP, vP, VP, DP).
CP	Complementizer phrase; the clausal projection of the head C. A phase in MP; Spec,CP is the landing site for wh-movement. C may be overt (<i>that, whether, if, for, . . .</i>) or null.
TP	Tense phrase; hosts tense and agreement features, with the surface subject in Spec,TP. T assigns nominative case in finite clauses. Not a phase in MP.
vP	Light-verb (little- <i>v</i>) phrase; the projection of v, which introduces the external argument in Spec,vP and merges with the VP below. A phase in MP when the light verb is transitive, written v* (projecting v*P; Chomsky 2001); all vPs in this paper are transitive v*Ps. Present in the infinitival and finite conditions but absent from the bare small clause.
VP	Lexical-verb phrase; contains the verb root and its internal complement(s). Not a phase; the sole verbal projection in the bare small clause.
DP	Determiner phrase; the nominal maximal phrase, covering subjects, objects, and wh-phrases.
Spec,XP	Specifier of XP; the structurally highest internal position of the phrase. In this paper: Spec,CP is the wh-phrase landing site, Spec,TP hosts the surface subject, and Spec,vP hosts the external argument (and intermediate wh-copies).
Phase	A cyclic spell-out domain. In MP English, v* and C are phase heads; vP and CP are the resulting phase domains. Once a phase is complete, its <i>complement</i> domain becomes inaccessible to higher operations; the head and specifier (the phase edge) remain accessible.
PIC	The domain of a phase head X is not accessible to operations outside the phase once the phase is complete; only X and the phase edge (specifier of XP) remain accessible. Long-distance movement must therefore proceed successive-cyclically through each phase edge — Spec,vP and Spec,CP in English.
Successive-cyclic movement	Wh-movement that halts at each intervening phase edge on the way to the matrix Spec,CP, as required by the PIC. Stops at Spec,CP are widely established; stops at Spec,vP are additionally proposed in Chomsky 2001 but not universally accepted.
Small clause	A minimal complement comprising only a VP and its subject; lacks TP and vP. E.g. the bracketed clause in “She saw [him eat the cake]”.
ECM	The matrix verb assigns accusative case to the subject of an infinitival complement across the clause boundary: e.g. <i>him</i> (not <i>he</i>) in “She expected <i>him</i> to leave”, because the infinitival T does not assign case.
Object control	The matrix object is co-indexed with a covert PRO subject of the embedded clause: e.g. “She persuaded him [PRO to leave]”. Unlike ECM, the embedded subject is PRO, not an overt DP.
Bridge verb	A matrix verb that permits long-distance wh-movement out of its CP complement (e.g. <i>think, claim, say</i>); contrasts with island-creating predicates that block movement.
Filler-gap dependency	The long-distance relation between a fronted wh-phrase (the filler) and the empty position (the gap) from which it was extracted.

C Detailed Phrase Structures

Figure 8 gives phrase structures with intermediate projections for all three conditions, showing the vP–VP decomposition under little-*v* and copy-theoretic lower copies for subject raising and head movement; intermediate wh-movement copies are omitted for clarity.

D Probe Training Quality

Figure 9 shows per-layer probe quality on the UD-EWT validation set for all 13 models. The textbook structural-probe profile — sharp rise from the embedding layer, plateau in the middle layers, and moderate decline near the output — holds consistently across all four architecture families, confirm-

ing that the probes underlying section 4 reliably encode dependency structure.

E Robustness Across Summary Metrics

Table 4 reports the WH-ESUBJ phase-count gradient under four summary statistics: per-contrast peak β , the effect at the canonical layer ($@L^*$), the layer median, and the fraction of FDR-significant positive layers ($\%_{\text{sig}+}$). The finite-bare contrast is robust across all four metrics in every model. The infinitival-bare contrast passes the peak criterion in all 13 models but attenuates substantially at canonical layer and median, reflecting its layer-localised character documented in section 4.1.

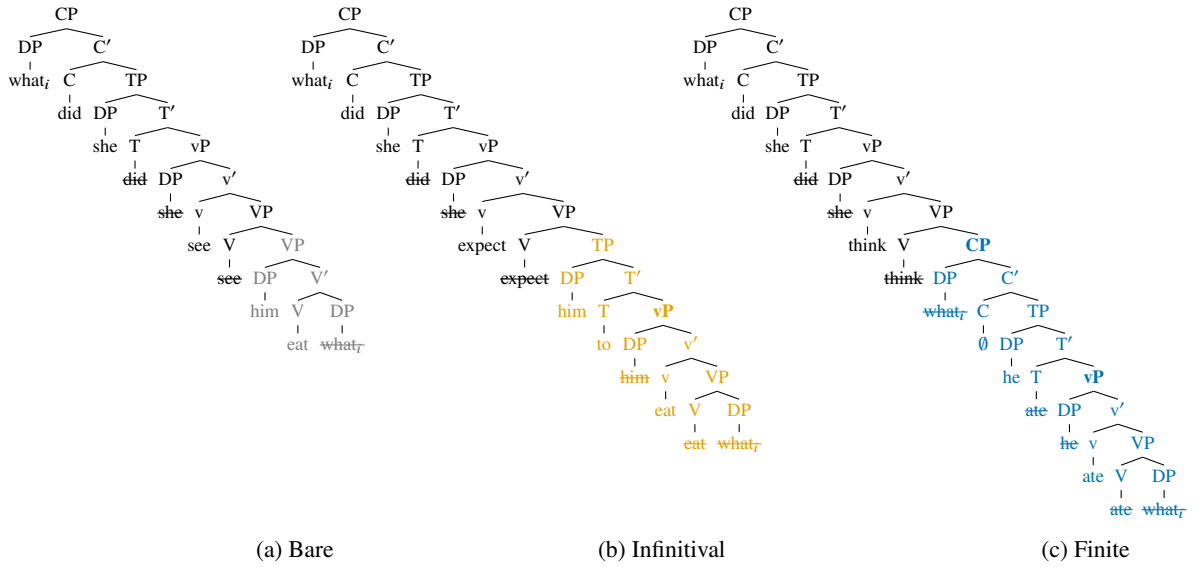


Figure 8: Phrase structures with intermediate projections for the three conditions, following copy theory (Chomsky, 2000). Struck-through nodes are lower (unpronounced) copies: the auxiliary *did* (C←T), subjects (Spec,TP←Spec,vP), and verbs (v ←V). The *wh*-element ($what_i$) is shown at its base position, at embedded Spec,CP (finite only), and at matrix Spec,CP; the intermediate copy at Spec,vP of the embedded clause is omitted for clarity. The embedded clause is colour-coded by condition; phase heads introduced within it are in **bold**: none in bare (a), the embedded vP in infinitival (b), the embedded CP and vP in finite (c).

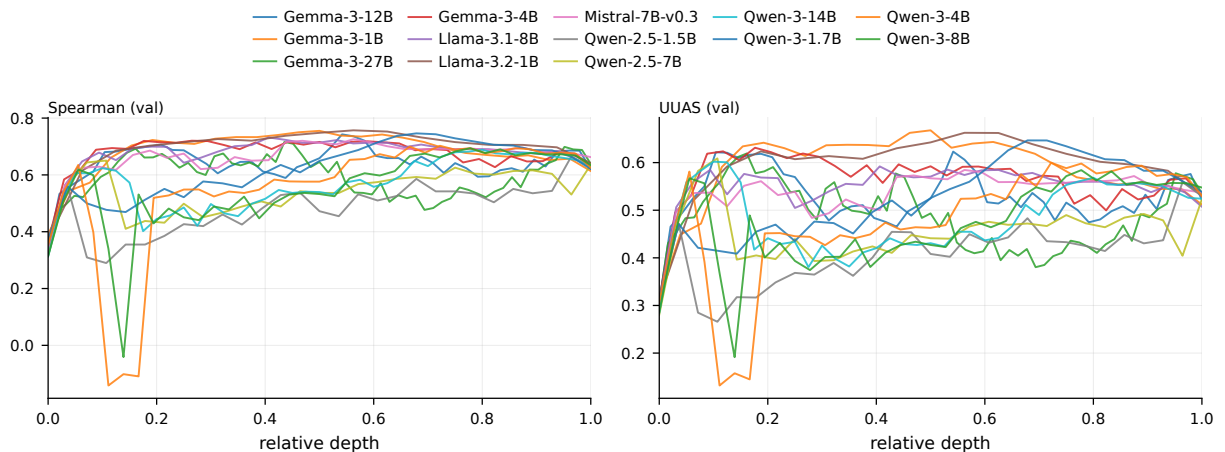


Figure 9: Per-layer probe quality on the UD-EWT validation set for all 13 models. Panel (a): distance Spearman correlation. Panel (b): undirected unlabelled attachment score (UUAS). The x -axis is relative depth (0 = embedding layer, 1 = final transformer block).

Table 4: Phase-count-gradient summary on the WH-ESUBJ pair under four metrics. “peak” is the per-contrast layer maximum; “@L*” is the effect at the canonical layer; “med” is the layer median; “%sig+” is the fraction of layers with a positive FDR-significant OLS estimate.

Model	L^*	finite – bare			infinitival – bare			
		peak	med	%sig+	peak	@L*	med	%sig+
Gemma-3-1B	4	+0.55	+0.09	63%	+0.15	+0.05	-0.10	33%
Gemma-3-4B	3	+0.91	+0.44	94%	+0.42	+0.07	+0.07	63%
Gemma-3-12B	29	+0.96	+0.43	98%	+0.37	+0.29	+0.03	51%
Gemma-3-27B	32	+0.99	+0.50	97%	+0.32	+0.10	-0.01	41%
Llama-3.2-1B	3	+0.77	+0.20	76%	+0.36	+0.12	+0.06	53%
Llama-3.1-8B	3	+0.72	+0.32	85%	+0.44	+0.18	+0.08	70%
Mistral-7B-v0.3	5	+0.73	+0.26	91%	+0.28	+0.20	+0.03	52%
Qwen-2.5-1.5B	1	+0.67	+0.12	69%	+0.57	+0.19	+0.06	52%
Qwen-3-1.7B	10	+0.82	+0.37	93%	+0.47	+0.27	+0.04	59%
Qwen-3-4B	10	+0.73	+0.43	95%	+0.34	-0.04	+0.02	51%
Qwen-2.5-7B	12	+0.88	+0.46	97%	+0.49	+0.17	+0.10	66%
Qwen-3-8B	10	+0.76	+0.40	97%	+0.28	+0.15	-0.04	32%
Qwen-3-14B	32	+0.89	+0.42	98%	+0.22	+0.18	+0.03	54%